Separation Science and Technology
Publication details, including instructions for authors and subscription information:
http://www.tandfonline.com/loi/lsst20

Propane/Propylene Separation by Simulated Moving Bed I. Adsorption of Propane, Propylene and Isobutane in Pellets of 13X Zeolite

Nabil Lamia [a b], Luc Wolff [b], Philibert Leflaive [b], Pedro Sá Gomes [a], Carlos A. Grande [a] & Alírio E. Rodrigues [a]

[a] Faculty of Engineering, Laboratory of Separation and Reaction Engineering (LSRE), Department of Chemical Engineering, University of Porto, Porto, Portugal

[b] Institut Français du Pétrole, IFP-Lyon Process Development and Engineering Division, Vernaison, France

Published online: 02 Oct 2007.

To cite this article: Nabil Lamia, Luc Wolff, Philibert Leflaive, Pedro Sá Gomes, Carlos A. Grande & Alírio E. Rodrigues (2007) Propane/Propylene Separation by Simulated Moving Bed I. Adsorption of Propane, Propylene and Isobutane in Pellets of 13X Zeolite, Separation Science and Technology, 42:12, 2539-2566, DOI: 10.1080/01496390701515219

To link to this article: http://dx.doi.org/10.1080/01496390701515219

Separation Science and Technology, 42: 2539–2566, 2007

ISSN 0149-6395 print/1520-5754 online
DOI: 10.1080/01496390701515219

Propane/Propylene Separation by Simulated Moving Bed I. Adsorption of Propane, Propylene and Isobutane in Pellets of 13X Zeolite

Nabil Lamia
Faculty of Engineering, Laboratory of Separation and Reaction Engineering (LSRE), Department of Chemical Engineering, University of Porto, Porto, Portugal and Institut Français du Pétrole, IFP-Lyon Process Development and Engineering Division, Vernaison, France

Luc Wolff and Philibert Leflaive
Institut Français du Pétrole, IFP-Lyon Process Development and Engineering Division, Vernaison, France

Pedro Sá Gomes, Carlos A. Grande, and Alírio E. Rodrigues
Faculty of Engineering, Laboratory of Separation and Reaction Engineering (LSRE), Department of Chemical Engineering, University of Porto, Porto, Portugal

Abstract: The separation of propane-propylene mixture is the most energy consuming operation in the petrochemical industry. Various studies have been investigated to relieve the cryogenic distillation ordinarily used for this separation, and the adsorption technology appeared to be a promising option. Considering the encouraging results obtained by cyclic adsorption processes and notably by pressure swing adsorption, the simulated moving bed (SMB) has been suggested as a new and competitive alternative. The keystone of a SMB for a gas mixture separation is the choice of an adequate and pertinent adsorbent-desorbent couple. In this work, isobutane has been tested as a potential desorbent over 13X zeolite. A gravimetric method has been used to measure

Received 18 March 2007, Accepted 3 May 2007
Address correspondence to Alírio E. Rodrigues, Faculty of Engineering, Laboratory of Separation and Reaction Engineering (LSRE), Department of Chemical Engineering, University of Porto, Rua Dr. Roberto Frias s/n, Porto 4200-465, Portugal. Tel.: 351 22 5081671; Fax: 351 22 5081674; E-mail: arodrig@fe.up.pt

the adsorption equilibrium isotherms of propylene, propane, and isobutane on 13X zeolite pellets over a temperature range from 333 K to 393 K and pressure up to 160 kPa. Experimental adsorption equilibrium isotherms were correlated with the Toth model. The 13X zeolite shows an intermediate loading capacity for isobutane at low pressures. Equilibrium capacities for propylene, propane, and isobutane at 373 K and 110 kPa were 2.12, 1.61, and 1.53 mol/kg, respectively. The heats of adsorption at zero coverage for propylene, propane, and isobutane were found to be 42.4, 36.9, 41.6 kJ/mol, respectively. Breakthrough curves of pure components were measured at 373 K and 150 kPa with different initial conditions (adsorbent bed saturated with nitrogen or isobutane). Experimental breakthrough curves were well-predicted by an exhaustive mathematical model taking into account the energy balance in the three phases (gas, solid, and wall column). Multi-component fixed bed adsorption experiments allowed us to observe that isobutane could displace an adsorbed propane/propylene mixture from the 13X zeolite and itself was fairly easily displaced from the adsorbent by this same mixture. These results confirmed the assumption that isobutane is a good desorbent for the adsorptive separation of C_3H_6/C_3H_8 mixture by a simulated moving bed.

Keywords: Propane, propylene, isobutane, 13X zeolite, adsorption equilibrium, fixed bed adsorption experiments, simulated moving bed

INTRODUCTION

Propylene is an important intermediate in the petrochemical industry and particularly for the production of polypropylene, acrylonitrile, isopropanol, cumene, and oxo alcohols. Propylene is mainly produced by steam cracking or by fluid catalytic cracking of heavy petroleum fractions and is generally obtained in a mixture with propane. But the propane-propylene gas separation is one of the most demanding energetic operation commercially practiced using cryogenic distillation (1–3). Due to the very close relative volatilities of the propane-propylene system (4), more than 150 theoretical plates are needed to achieve polymer-grade propylene (purity of $>$99.5%). A number of alternative methods have been investigated to reduce the operational costs and cyclic adsorption processes appeared to be a promising option (5, 6). The pressure swing adsorption (PSA) and the vacuum swing adsorption (VSA) processes based on zeolite molecular sieves have been proposed as a possible approach. These processes have been widely discussed in the literature (7–10) showing an interesting product recovery (87%) with a very high purity (99%). Nevertheless, other adsorption processes seem to be suitable for the separation of the propane-propylene mixture and particularly the simulated moving bed.

The simulated moving bed (SMB) technology is currently receiving an increasing interest as an alternative technique for the separation of gas mixtures. Concisely, the SMB technology allows the continuous injection and separation of binary mixtures. The simulated countercurrent contact

between the solid and fluid phase maximizes the mass transfer driving force. The SMB process is well known in large-scale petrochemical industry, where the Sorbex technology has been applied since the 1960s in a number of processes (11). In all of these, the continuous counter-current flow of the fluid and of the solid adsorbent is simulated by periodically switching the different inlets and outlets in an adsorbent column divided into a number of fixed beds. Recently, a process similar to an SMB adsorber has been studied by Rao et al. to separate propane-propylene mixture (12). Contrary to the conventional SMB, this process uses pressure swing to regenerate the solid adsorbent.

The main objective of this work is to come upon an interesting adsorbent-desorbent couple to operate a propane-propylene separation with a SMB. In the literature, a number of commercial sorbents have been tested to separate C_3 components, such as 5A and 4A zeolites (13, 14) or more recently new sorbents using π-complexing agents (15). Nevertheless, to achieve our objective zeolite 13X was chosen as a solid adsorbent for this study based on its capacity and adequate kinetic behavior for the separation of this system (16). As literature data at appropriate temperature are poor and incomplete, additional single adsorption isotherms of propylene (C_3H_6), propane (C_3H_8), and isobutane (iC_4H_{10}) over commercial 13X zeolite have been measured at temperatures between 333 and 393 K and pressure up to 160 kPa using a gravimetric method. Since the 13X zeolite is very difficult to regenerate using a pressure swing due to the almost irreversible nature of the adsorption isotherms, the choice of the desorbent is extremely important. According to the literature (17, 18) and in conformity with the industrial constraints, isobutane has been selected as a potential desorbent able to readily displace the adsorbed gas mixture from the adsorbent. To confirm this choice, fixed bed adsorption experiments were carried out at 373 K with two different initial conditions regarding the saturation of the adsorbent bed. The first strategy was to perform single component breakthrough curves with an adsorbent bed initially activated by an inert gas like nitrogen. The second way was to saturate it originally with the chosen desorbent, allowing us to carry out breakthrough (feed is propane or propylene) and reverse breakthrough experiments (after complete breakthrough of propane or propylene, isobutane is injected). This last strategy has also been applied to study the adsorption and desorption of a propane-propylene mixture over a column packed with 13X zeolite saturated by isobutane. A patent is pending on the choice of 13X zeolite/Isobutane as an ideal adsorbent-desorbent couple for the separation of the propane-propylene mixture by adsorption in simulated moving bed (19). The design of a SMB unit requires the development of a model that can describe the dynamics of adsorption on a fixed bed, taking into account all the relevant transport phenomena. In this work a mathematical model of a nonisothermal, nonadiabatic fixed bed adsorber has been developed and tested with the breakthrough curves obtained experimentally.

EXPERIMENTAL SECTION

Single-adsorption Equilibrium Isotherms

Adsorption equilibrium of pure gases was performed in a magnetic suspension microbalance (Rubotherm, Bochum, Germany) operated in a closed system mode. The experimental installation used for the adsorption measurements is shown in Fig. 1.

A defined amount of adsorbent extrudates ($\cong$10 g wet sample) is placed in a basket suspended by a permanent magnet through an electromagnet. The sample was submitted to a controlled temperature ramp of 2 K.min^{-1} in vacuum conditions until 593 K was reached. Activation of the sample was carried out under this temperature and 1 mbar pressure during 10 h. The adsorbent lost nearly 20% of its weight during the activation step. The pure gas was then fed through tubing equiped with a valve, from the gas cylinder to the magnetic balance. Pressure and temperature in the measuring cell were measured with a Lucas Schaevitz transducer with an accuracy $\pm 5 \times 10^{-2}$ kPa and an Omega thermocouple with an accuracy ± 0.1 K, respectively. All measured data (mass change, pressure, and temperature)

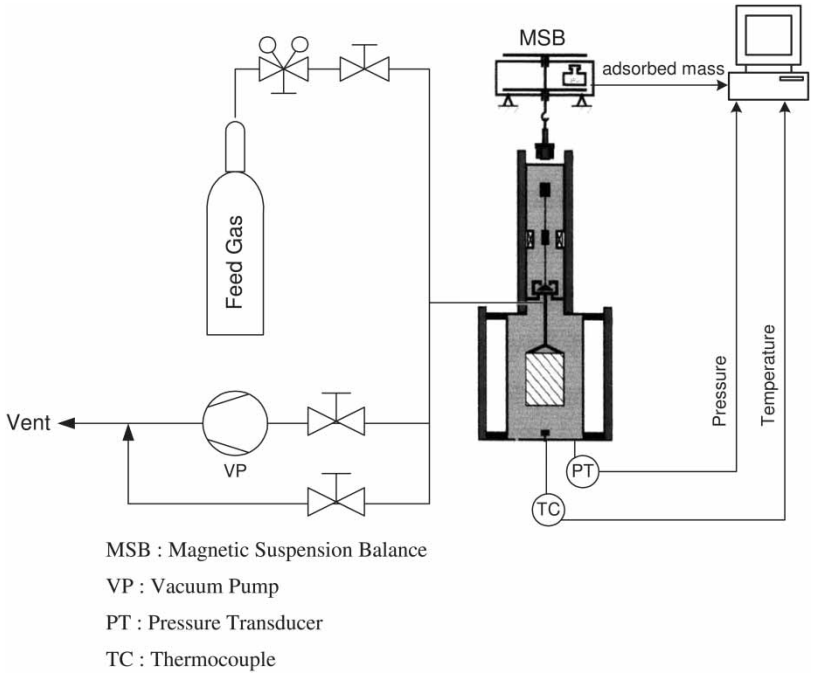

Figure 1. Schematic diagram of the experimental installation used for the adsorption isotherms measurements.

Table 1. Physical properties of 13X zeolite (CECA)

Parameters	Value	Unit
Extrudate radius (R_p)	0.8	mm
Crystal radius (r_c)	1.0	μm
Macropore radius (r_p)	0.17	μm
Pellet density (ρ_p)	1357	kg/m^3
Pellet porosity (ε_p)	0.395	—

were recorded by a personal computer. Adsorption equilibrium isotherms were measured at 333, 353, 373, 393 K in the range of 0 to 160 kPa.

13X zeolite extrudates were provided by CECA (France) and Table 1 shows some of their physical properties. All gases were provided by Air Liquide: The purity of the sorbate gases used was N24 for propylene (>99.4%), N35 for propane (>99.95%), and N35 for isobutane (>99.95%).

The experimental adsorption equilibrium data were fitted with the Toth Model (20):

$$q_i = q_{m,i}\frac{b_i P}{\left[1+(b_i P)^{k_i}\right]^{1/k_i}} \tag{1}$$

$$b_i = b_{i,0} exp\left(\frac{-\Delta H_i}{\Re T}\right) \tag{2}$$

where q_i is the absolute adsorbed amount of the single component i, $q_{m,i}$ is the maximum loading capacity of the sorbent, b_i is the affinity parameter of the pure component i for the solid sorbent, ΔH_i is the isosteric heat of adsorption at zero loading, and $k_i = A_i + D_i T$ is the solid heterogeneity parameter (21).

Fixed Bed Adsorption Experiments

The experimental set-up has three main sections:

i. a feed section which allows the constitution of different studied gases mixtures
ii. an adsorption column in a convective air furnace and
iii. an analytical section arranged around a gas chromatograph (GC).

This equipment allows to work with pure gas or with gas mixtures of three components. The apparatus can work with pressures ranging from 0.1 to 5 bar, and temperatures between 303 and 673 K, and with feed flowrates ranging from 0.1 to 6 SLPM (273 K and $1.01325 \cdot 10^5$ Pa). Gas analysis is carried out with an on-line gas chromatograph with a FID detector and

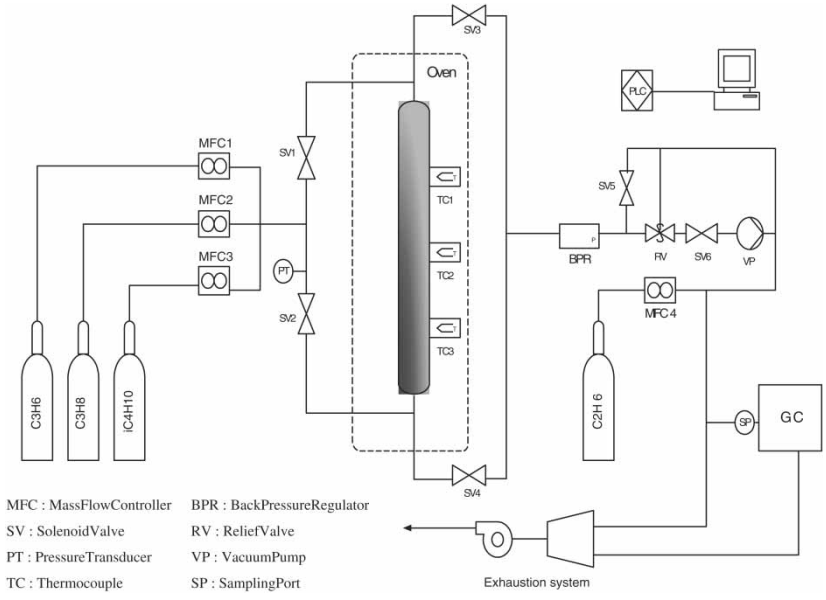

Figure 2. Schematic diagram of the experimental set-up used for the breakthrough experiments.

coupled with an automatic sampler. The apparatus is controlled and data are recorded through a computer program interface. The column is in stainless steel with a diameter of $2.14\ 10^{-2}$ m and is 0.84 m long. Three K-type thermocouples were located at 0.17, 0.43, and 0.67 meter from the feed inlet of the column, measuring the gas temperature at the bottom and the middle of the column while the thermocouple placed at the top measures the wall column temperature. Figure 2 shows the experimental set-up used for mono and multicomponent breakthrough curves. Bed characteristics are given in Table 2.

Before performing any adsorption experiment the solid was activated at high temperature. The solid was dried in-situ, inside the column in the convective furnace of the installation. A temperature of 593 K was fixed an inert gas (nitrogen) flow between 30 to 50 $\text{ml} \cdot \text{min}^{-1}$ at laboratory scale conditions

Table 2. Characteristics of the fixed bed column

Parameters	Value	Unit
Bed radius (R_w)	1.07×10^{-2}	m
Bed length (L)	0.84	m
Bed porosity (ε_b)	0.39	—
Bulk density (ρ_b)	820	$\text{kg} \cdot \text{m}^{-3}$
Wall density (ρ_w)	8238	$\text{kg} \cdot \text{m}^{-3}$

Table 3. Experimental conditions for the runs performed for single and multi-components

Figure	Initial bed saturation	$y_{C_3H_6}$	$y_{C_3H_8}$	$y_{iC_4H_{10}}$	Q (SLPM)	P_0 (bar)	T_0 (K)
6a, 6b	N_2	1.0	0.0	0.0	1.0	1.5	373
7a, 7b	N_2	0.0	1.0	0.0	1.0	1.5	373
8a, 8b	N_2	0.0	0.0	1.0	1.0	1.5	373
10a, 10b	iC_4H_{10}	1.0	0.0	0.0	1.0	1.5	373
11a, 11b	C_3H_6	0.0	0.0	1.0	1.0	1.5	373
12a, 12b	iC_4H_{10}	0.0	1.0	0.0	1.0	1.5	373
13a, 13b	C_3H_8	0.0	0.0	1.0	1.0	1.5	373
14a, 14b	iC_4H_{10}	0.75	0.25	0.0	1.0	1.5	373
15a, 15b	C_3H_6–C_3H_8	0.0	0.0	1.0	1.0	1.5	373

Note: Q is the volumetric flow in SLPM at standard conditions (273.15 K, 1.01325 10^5 Pa).

were selected for a period of 18 hours. The heating of the column was performed with a ramp of $2\ K \cdot min^{-1}$, that was introduced in the furnace temperature controller. Once the column was prepared and fixed at the operating temperature and the controller equipment and GC were ready for work, the adsorbent was saturated with an inert gas or with isobutane. Then, single component breakthrough experiment was started by injecting the adsorbate in the column with a volumetric flowrate of 1.0 SLPM at 373 K and 150 kPa. Finally a ternary system comprising a mixture of propane and propylene was also studied through a fixed bed adsorbent saturated with isobutane. It should be noted, that single and multicomponent desorptions were performed in the same way. The experimental conditions for all the adsorption experiments carried out with propane, propylene, and isobutane as a desorbent are listed in Table 3.

THEORETICAL SECTION

Mathematical Modeling of Fixed Bed Adsorption

The mathematical model used to describe the dynamic behavior of the fixed bed adsorber is derived from mass and energy balances considering the following assumptions:

1. Ideal gas law applies;
2. The total pressure is constant during the sorption process;
3. The flow pattern is described by the axial dispersed plug flow model;
4. The system is a nonisothermal and nonadiabatic column packed with 13X zeolite;

Table 4. Usual dimensionless numbers

Biot	$B_i = R_p\, K_{m,i}/5\varepsilon_p\, D_{p,i}$
Reynolds	$Re = \rho_i\, v_s\, d_p/\mu_0$
Schmidt	$Sc = \mu_0/\rho_i\, D_{m,i}$
Sherwood (23)	$Sh = 2.0 + 1.1Re^{1/6}Sc^{1/3}$
Prandtl	$Pr = \hat{C}_{pg}\, \mu_0/k_g$
Nusselt (23)	$Nu = 2.0 + 1.1Re^{1/6}\, Pr^{1/3}$
Peclet (mass)	$Pe_m = v_0 \cdot L/\varepsilon_b\, D_{zm}$
Peclet (heat)	$Pe_h = C_{i,0}\, \tilde{C}_p\, v_0 \cdot L/\lambda$
Stanton (gas-solid)	$St^v_{gs} = (1-\varepsilon)\, a\, h_f\, \tau_0/\varepsilon_b\, C_o\, F\tilde{C}_v$
Stanton (gas-wall)	$St^v_{gw} = 2\, h_w\, \tau_0/R_w\, \varepsilon_b\, C_o\, F\, \tilde{C}_v$

5. The mass transfer rate can be represented by a linear driving force (LDF) rate expression;
6. Constant cross section area. The void fraction is uniform in the column.

Note that all the following equations are expressed in dimensionless terms and the usual dimensionless numbers are listed in the Table 4.

Based on the above assumptions, the mass balance for each component of the mixture and the total mass balance were written as follows, where F_i is the dimensionless concentration in the bulk normalized by the total mole concentration at the feed condition C_0, $\bar{f}_i$ is the dimensionless average concentration in the particle pores, also normalized by C_0 and $g_i^{=} = n_i^{=}/q_{m,i}$ is the dimensionless average adsorbed concentration for i component in the pellet, $\bar{g}_i^*$ is adsorbed phase concentration in the crystal in equilibrium with the gas inside the particle.

Mass Balance of Component i in the Bulk Fluid

$$\frac{\partial F_i}{\partial \theta} = \frac{\partial}{\partial \zeta}\left(\frac{v^*}{Pe_m}\frac{\partial F_i}{\partial \zeta}\right) - v^*\frac{\partial F_i}{\partial \zeta} - F_i\frac{\partial v^*}{\partial \zeta} - \tau_o\frac{(1-\varepsilon_b)}{\varepsilon_b}\frac{aK_{m,i}}{(Bi_{m,i}+1)}(F_i - \bar{f}_i) \tag{3}$$

where $\theta = t/\tau_o$ is the dimensionless time normalized by the space time $\tau_o = \varepsilon_b L/v_o$, $\zeta = z/L$ is the dimensionless column axial coordinate, v^* is the dimensionless superficial velocity, Pe_m and Bi_m are the mass Peclet number and the Biot number respectively defined in Table 4, ε_b is the bed porosity, K_m is the mass transfer coefficient, a is the specific surface area of the adsorbent particle.

Overall Mass Balance

$$\frac{\partial F}{\partial \theta} = -\frac{\partial (v^* F)}{\partial \zeta} - \tau_o\frac{(1-\varepsilon_b)}{\varepsilon_b}\frac{aK_m}{(Bi_m+1)}(F - \bar{f}) \tag{4}$$

It is worthwhile to note that in the definition of the dimensionless concentrations, the total fluid phase concentration has been used in order to obtain $0 \le F_i \le 1$ and $0 \le \bar{f}_i \le 1$ to enable the model to describe both adsorption and desorption operations.

Mass Balance Inside the Pellet for Component i

$$\frac{\partial \bar{f}_i}{\partial \theta} = N_p \frac{Bi_{m,i}}{(Bi_{m,i}+1)}(F_i - \bar{f}_i) - \gamma_i \frac{\partial \bar{\bar{g}}_i}{\partial \theta} \quad \text{with} \quad N_{p,i} = \frac{15 D_{p,i}\tau_0}{R_p^2} \quad \text{and} \quad \gamma_i = \frac{\rho_p q_{m,i}}{\varepsilon_p C_o} \tag{5}$$

where $D_{p,i}$ is the pore diffusivity for the component i, ρ_p is the pellet density, ε_p is the pellet void fraction, and $q_{m,i}$ is the loading saturation coefficient of the sorbent for each adsorbed component and R_p is the pellet radius.

Mass Balance Inside the Crystal for Component i

$$\frac{\partial \bar{\bar{g}}_i}{\partial \theta} = N_c(\bar{g}_i^* - \bar{\bar{g}}_i) \quad \text{with} \quad N_{p,i} = \frac{15 D_{c,i}\tau_0}{r_c^2} \tag{6}$$

where $D_{c,i}$ is the crystal diffusivity for the component i, and r_c is the crystal radius.

Toth Multicomponent Adsorption Equilibrium Isotherm

$$\bar{g}_i^* = \frac{b_i \bar{f}_i C_0 \Re T_s^* T_0}{\left(1 + \sum_{i=1}^{N} (b_i \bar{f}_i C_0 \Re T_s^* T_0)^k\right)^{1/k}} \tag{7}$$

Heterogeneous Energy Balance

The energy balance takes into account the three phases (gas, solid, and wall column) separately. In this way, one independent energy balance is formulated for each phase and then coupled to each other through film energy transfer terms.

The energy balance in the gas phase expressed below, gives the variation of gas temperature with time in terms of dimensionless variables:

$$\frac{\partial T_g^*}{\partial \theta} = \frac{1}{\tilde{C}_v F}\frac{\partial}{\partial \zeta}\left(\frac{\tilde{C}_p v^*}{Pe_h}\frac{\partial T_g^*}{\partial \zeta}\right) - v^* \frac{\tilde{C}_p}{\tilde{C}_v}\left(\frac{\partial T_g^*}{\partial \zeta}\right) + \frac{\Re T_g^*}{\tilde{C}_v F}\left(\frac{\partial F}{\partial \theta}\right) - St_{gs}^v (T_g^* - T_s^*) - St_{gw}^v (T_g^* - T_w^*) \tag{8}$$

where $\tilde{C}_v$ is the molar specific heat at constant volume of the gas mixture, $\tilde{C}_p$ is

the molar specific heat at constant pressure of the gas mixture, Pe_h is the thermal Peclet number, St^v_{gs} is the Stanton number between the bulk gas and the pellet, and St^v_{gw} is the Stanton number between the bulk gas and the column wall.

Considering a pellet as control volume, energy balance in the solid phase can be written with dimensionless parameters as follows:

$$\frac{\partial T^*_s}{\partial \theta} = B_f T^*_s \frac{\partial \bar{f}}{\partial \theta} + \sum_{i=1}^{n} B_i \frac{\partial \bar{\bar{g}}_i}{\partial \theta} + B_{gs}(T^*_g - T^*_s) \tag{9}$$

where B_f, B_i, and B_{gs} are dimensionless terms defined below:

$$B_f = \frac{(1-\varepsilon)\varepsilon_p \Re T_0 C_0}{B\tau_o} \quad B_i = \frac{(-\Delta H_i)\rho_b q_{mi}}{B\tau_o} \qquad B_{gs} = \frac{(1-\varepsilon_b)h_f\ aT_o}{B} \tag{10a}$$

with

$$B = \frac{T_o(1-\varepsilon_b)}{\tau_o}\left\{\varepsilon_p C_o \sum_{i=1}^{n} \bar{f}_i \tilde{C}_{v,i} + \rho_p q_m \sum_{i=1}^{n} \bar{\bar{g}}_i \tilde{C}_{v,ads.i} + \rho_p \hat{C}_{ps}\right\} \tag{10b}$$

where ρ_b is the bulk density, ΔH_i is the isosteric heat of adsorption of the component i, $\tilde{C}_{v,ads,i}$ is the molar specific heat of the component i adsorbed at the solid phase which is considered equal to $\tilde{C}_{v,i}$, and $\hat{C}_{ps}$ is the mass specific heat of the solid. (Note that B is expressed in $\mathrm{W/m^3}$)

Finally, the set of energy balances is completed with the wall energy balance that can be expressed also as function of dimensionless variables:

$$\frac{\partial T^*_w}{\partial \theta} = B_{w1}(T^*_g - T^*_w) - B_{w2}(T^*_w - T_\infty) \tag{11}$$

where

$$B_{w1} = \frac{\tau_0 \alpha_w h_w}{\rho_w \hat{C}_{pw}}$$

and

$$B_{w2} = \frac{\alpha_{wl} U}{\rho_w \hat{C}_{pw}},$$

with

$$\alpha_w = \frac{D_w}{e(D_w + e)}$$

the ratio of the internal surface area to the volume of the column wall,

$$\alpha_{wl} = \frac{D_w}{(D_w + e)ln((D_w + e)/D_w)}$$

is the ratio of the logarithmic mean surface area of the column shell to the volume of the column wall, D_w is the column inside diameter, e the thickness of shell, h_w is the heat convective coefficient between the gas and the wall, ρ_w and $\hat{C}_{pw}$ are the density and the specific heat of the column shell and U is a global external heat transfer coefficient.

Variable Superficial Velocity of the Gas Mixture along the Bed

The formulation of the dimensionless velocity along the bed is derived from the global mass balance and the energy balance in the gas phase. Substituting eq. (8) in eq. (4) after applying the ideal gas law in each equation, it follows:

$$\begin{aligned}\frac{\partial v^*}{\partial \zeta} = &-\frac{1}{F}\sum_{i=1}^{n} \tau_o \frac{(1-\varepsilon_b)}{\varepsilon_b}\frac{aK_{m,i}}{(Bi_{m,i}+1)}(F_i - \bar{f}_i) \\ &- St^p_{gs}\left(1 - \frac{T^*_s}{T^*_g}\right) - St^p_{gw}\left(1 - \frac{T^*_w}{T^*_g}\right)\end{aligned} \tag{12}$$

It may be well worth pointing out that the Stanton numbers are expressed in this equation with respect to the molar specific heat at constant pressure $\tilde{C}_p$.

At time zero the inert gas is flowing at feed temperature without any adsorbed species in the solid phase; in dimensionless terms we get:

$$\theta = 0, \forall \zeta \quad F_i = \bar{f}_i = \bar{\bar{g}}_i = 0 \quad v^* = 1 \quad T^*_g = T^*_s = T^*_w = 1.0 \tag{13}$$

In the case of a fixed bed column saturated with an active adsorbate as isobutane with molar fractions $y_{i,0}$, the set of initial conditions can be replaced by:

$$F_i = \bar{f}_i = \bar{\bar{g}}_i = y_{i,0} \tag{14}$$

The Danckwerts boundary conditions at the column inlet ($\zeta = 0$) and column exit ($\zeta = 1$) for $\theta > 0$ are:

$$\begin{aligned}\zeta = 0, \quad &-\frac{1}{Pe_m}\left.\frac{\partial F_i}{\partial \zeta}\right|_{\varsigma=0} + (F_i - F_{i,0}) = 0 \quad \text{and} \\ &-\frac{1}{Pe_h}\left.\frac{\partial T^*_g}{\partial \zeta}\right|_{\varsigma=0} + (T^*_g - T^*_{g,0}) = 0\end{aligned} \tag{15}$$

$$\zeta = 1, \quad \left.\frac{\partial F_i}{\partial \zeta}\right|_{\varsigma=1} = 0 \quad \text{and} \quad \left.\frac{\partial T^*_g}{\partial \zeta}\right|_{\varsigma=1} = 0 \tag{16}$$

Methodology and Estimation of Transport Parameters used in the Model

Molecular diffusivities are calculated with Chapman-Enskog equation and pore diffusivities are estimated using Bosanquet relationship. Gas specific heat, gas viscosity, and gas heat conductivities are temperature and pressure dependent, being calculated using methods and thermodynamic data found in Reid et al. (22)

The mass transfer coefficient $K_{m,i} = (Sh_i \cdot D_{m,i})/d_p$ and the heat convective coefficient $h_f = (N_u \cdot k_g)/d_p$ were followed from the correlations proposed by Wakao and Funazkri (23), where d_p is the pellet diameter, Sh_i and Nu are the Sherwood and the Nusselt number for the single component i respectively, and defined in Table 4.

The mass axial dispersion coefficient D_{zm} used in the mass Peclet number was estimated from the correlation of Wakao and Funazkri (23):

$$D_{zm} = \frac{D_{m,i}}{\varepsilon_b}(20 + 0.5\ Sc_i\ Re_i) \tag{17}$$

In the same way, the heat axial dispersion coefficient λ used in the thermal Peclet number was estimated from an analogous correlation:

$$\lambda = k_g(7 + 0.5 Pr_i Re_i) \tag{18}$$

where Sc_i, Re_i, and Pr_i are the Schimdt number, the Reynolds particle number and Prandtl number for the component i, respectively (see Table 4)

The value of the overall heat transfert coefficient, U, and the wall specific heat, $\hat{C}_{pw}$, were set to $30\ \mathrm{W/m^2 \cdot K}$ and $500\ \mathrm{J \cdot kg^{-1} \cdot K^{-1}}$, respectively. These values have been reported by Da Silva and Rodrigues (7) to describe the heat transfer between a stainless column (similar to the one used in this work) and the external air in a convective furnace. Regarding the heat wall transfer coefficient, h_w, this parameter was found by fitting the simulation breakthrough curves to experimental data.

Assuming N components in the mixture, there are $3N + 4$ unknowns in the model; the dimensionless concentration in the bulk F_i (ζ θ), the dimensionless average concentration in the particle pores $\bar{f}_i$ (ζ, θ), the dimensionless average adsorbed concentration in the pellet $\bar{g}_i(\zeta, \theta)$ for each component, and the dimensionless superficial velocity v^* (ζ, θ). Then, we have the dimensionless gas temperature $T_g{}^*$ (ζ, θ), the dimensionless solid temperature $T_s{}^*$ (ζ, θ) and the dimensionless wall temperature $T_w{}^*(\zeta, \theta)$ corresponding to the energy balance. The last equation necessary to evaluate all the unknowns, is a stoichiometric equation:

$$\sum_{i=1}^{N} \frac{F_i}{\rho_i^*} = 1 \quad \text{with} \quad \rho_i^* = \frac{\rho_i}{C_0} \tag{19}$$

where $\rho_i{}^*$ is the dimensionless molar density of the pure ith component. In this

study, the molar densities of propane, propylene and isobutane are equals and closed to C_0. Thus, the dimensionless concentration in the bulk of the Nth component can be evaluated as follows:

$$F_N = \rho_N^* \left(1 - \sum_{i=1}^{N-1} \frac{F_i}{\rho_i^*} \right) \cong 1 - \sum_{i=1}^{N-1} F_i \tag{20}$$

With this last equation the mathematical model is complete. It is thus constituted by a parabolic system of $3N + 4$ partial differential equations.

Finally, it should be noted that these model equations (except the equation of velocity along the bed) have been proposed following the work of Da Silva and Rodrigues (24). The mathematical model involves a system of partial differential and algebraic equations (PDAEs). The axial domain was discretized by using orthogonal collocation method in finite elements (OCFEM); third order polynomials were used in the 50 finite elements. The system of ordinary differential and algebraic equation (ODAEs) was integrated over time using the DASOLV integrator. For all simulations a tolerance equal to 10^{-5} was fixed.

RESULTS AND DISCUSSION

Adsorption Isotherms of Pure Components on 13X Zeolite

Pure component adsorption isotherms of propylene, propane, and isobutane on zeolite 13X at 333, 353, 373, and 393 K are shown in Figs. 3, 4, and 5. The

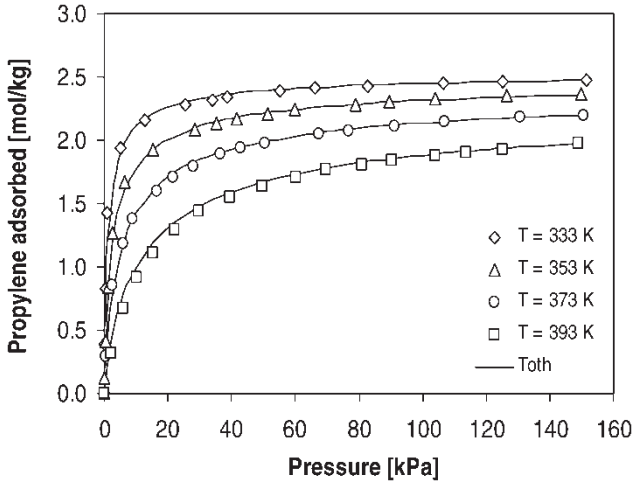

Figure 3. Propylene adsorption equilibrium over 13X zeolite at different temperatures. The solid line is the Toth model.

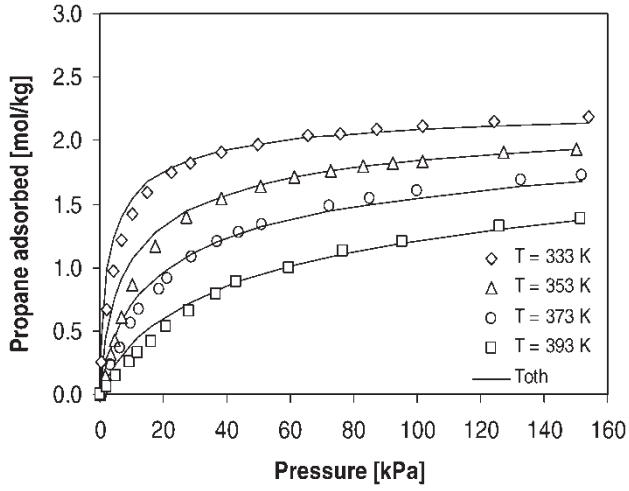

Figure 4. Propane adsorption equilibrium over 13X zeolite at different temperatures. The solid line is the Toth model.

fitting obtained with the Toth model is represented with solid lines in those figures. The values of the fitting parameters obtained with the Toth isotherm that was adjusted over the experimental data are reported in Table 5. It is noted particularly that heats of adsorption at zero coverage for propylene, propane, and isobutane are found to be 42.4, 36.9, 41.6 kJ/mol, respectively. The experimental results of the three gases are well-correlated with this

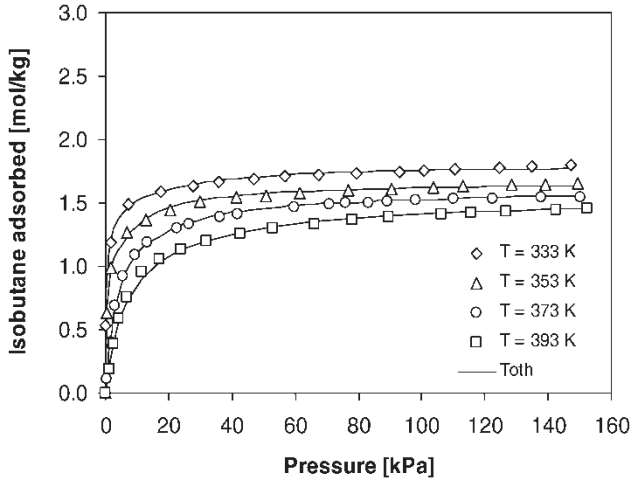

Figure 5. Isobutane adsorption equilibrium over 13X zeolite at different temperatures. The solid line is the Toth model.

Table 5. Fitting parameters of the toth model

Gas	$q_{m,i}$ (mol/kg)	$b_{i,0}$ (kPa^{-1})	$-\Delta H_i$ (kJ/mol)	A_i (−)	D_i (K^{-1})
Propylene	2.59	$2.5 \cdot 10^{-7}$	42.4	0.658	0.0
Propane	2.20	$2.5 \cdot 10^{-7}$	36.9	0.892	0.0
Isobutane	1.78	$2.5 \cdot 10^{-7}$	41.6	0.848	0.0

model. In Table 6 is listed the absolute average deviation (AAD) between experimental data and correlated results. For all pressures and at any temperatures, propylene is the most adsorbed gas. This larger capacity for propylene with respect to propane has been observed by Da Silva and Rodrigues (26). On the other hand it should be noticed that the isobutane adsorption equilibrium isotherms measured in this work are in reasonable agreement with the measurements performed at 373 K by Hyun and Danner (17). Furthermore, regarding isobutane, it can be observed at low pressures that its loading capacity is intermediate to propylene and propane. Another way to point out the intermediate aspect of isobutane with respect to C_3 components is to calculate the selectivity factor as the ratio $S_{\text{isobutane,C3}} = b_{\text{isobutane}}/b_{\text{C3}}$. A value around 4.5 is found for the system isobutane-propane while 0.8 is obtained for the couple isobutane-propylene at 373 K. Considering this observation, isobutane could be used in a simulated moving bed process as a possible desorbent. However, in order to confirm the intermediate nature of isobutane, some breakthrough experiments are necessary to study the dynamic behavior of propane and propylene in the presence of isobutane in a column packed with 13X zeolite.

Fixed Bed Adsorption of Single Component over 13X Zeolite Activated by Nitrogen

In order to describe the fixed bed dynamics of the adsorption of propane, propylene, and their mixture with isobutane, the basic information required is the adsorption of these pure gases over a fixed bed adsorbent activated

Table 6. Absolute average deviation (AAD) between experimental data and correlated results (%)

Temperature (K)	Propylene	Propane	Isobutane
333	2.82	4.37	0.83
353	2.72	6.36	1.64
373	1.33	5.92	3.39
393	3.19	8.17	2.61

Note: AAD (%) = $\sum$|exp.-cal.|/exp. × 100/No. of exp.

with an inert gas. The breakthrough curves obtained for each single component were simulated with the model proposed in the previous section, using the Toth parameters to describe the adsorption equilibrium. The values of the physical and transport properties of each gas used for the simulation are shown in Table 7. Figures 6, 7, and 8 show the exit molar flowrate breakthrough curves of propylene, propane, and isobutane respectively, as well as the gas and wall temperature histories at the middle and the top of the column. It is observed that the model reproduces the experimental data satisfactorily for the different pure components and the gas temperature histories are in good agreement with the heats of adsorption determined previously. Nevertheless, it should be noted that the thermocouple inserted at the column top hardly measures only the shell, and the simulated wall column temperature cannot perfectly match the experimental data.

Figure 9 shows the dimensionless adsorbed phase concentration $\bar{\bar{g}}$ and the equilibrium values $\bar{g}^*$ for isobutane. It is observed that dimensionless adsorbed solid concentration and the respective equilibrium values are approximately the same. Therefore, considering this simulation, it can be concluded that the macropore resistance is higher than micropore resistance. Another way to demonstrate that macropore mass transfer is the controlling mechanism is to use Ruthven and Loughlin criterion (27–29), written as:

$$\Gamma = \frac{(D_c/r_c^2)(1+K)}{(D_p/R_p^2)} \tag{21}$$

where $K = (1-\varepsilon_p)H/\varepsilon_v$ is the capacity factor and H the slope of the

Table 7. Calculated parameters used in the mathematical model for single component breakthrough curves

Parameters	C_3H_6	C_3H_8	iC_4H_{10}	Unit
D_c (25)	$2.69 \cdot 10^{-11}$	$1.55 \cdot 10^{-11}$	$1.58 \cdot 10^{-11}$	$m^2 \cdot s^{-1}$
D_p	$5.74 \cdot 10^{-6}$	$5.45 \cdot 10^{-6}$	$5.14 \cdot 10^{-6}$	$m^2 \cdot s^{-1}$
D_{zm}	$10.49 \cdot 10^{-4}$	$9.98 \cdot 10^{-4}$	$9.73 \cdot 10^{-4}$	$m^2 \cdot s^{-1}$
K_m	$4.56 \cdot 10^{-2}$	$4.39 \cdot 10^{-2}$	$4.51 \cdot 10^{-2}$	$m \cdot s^{-1}$
k_g	$3.34 \cdot 10^{-2}$	$2.77 \cdot 10^{-2}$	$3.11 \cdot 10^{-2}$	$W \cdot m^{-1} \cdot K^{-1}$
λ	0.46	0.38	0.51	$W \cdot m^{-1} \cdot K^{-1}$
h_f	98.8	83.5	107	$W \cdot m^{-2} \cdot K^{-1}$
B_i	4.98	5.05	5.52	—
Re	14.77	15.51	20.47	—
Sc	0.59	0.60	0.47	—
Sh	6.65	6.81	7.22	—
Pr	0.89	0.88	0.92	—
Nu	7.33	7.64	8.54	—
Pe_m	122	128	131	—
Pe_h	356	365	382	—

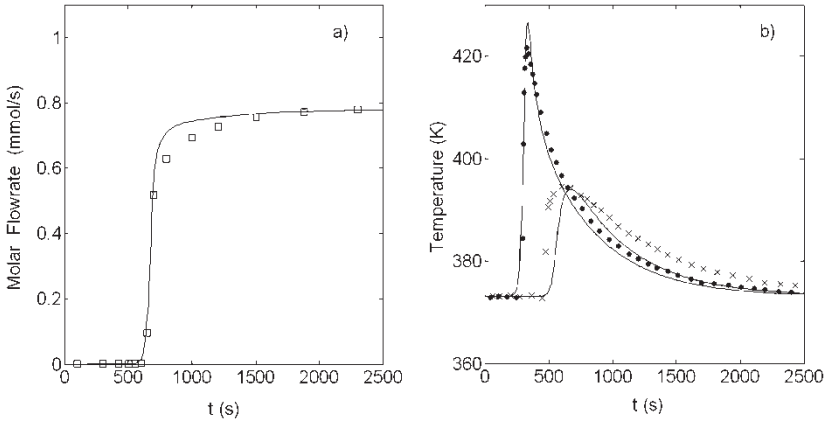

Figure 6. a) Experimental breakthrough curves of pure propylene (□) on 13X zeolite initially activated with nitrogen; b) gas temperature histories at the middle bed (●) and wall column temperature histories at the top bed (×) during the adsorption of propylene. Solid lines are simulations obtained with the non-isothermal bidisperse model. ($Q = 1.0$ SLPM; $P = 1.5$ bar; $T = 373$ K).

considered isotherm at the origin. Macropore diffusion is the controlling mechanism for $\Gamma > 10$, while for $\Gamma < 0.1$ the micropore diffusivity is the dominant mass transfer mechanism. In the case of isobutane adsorption over 13X zeolite at 373 K, we found $\Gamma > 500$. This result confirms the previous conclusion made from the simulations regarding the macropore control.

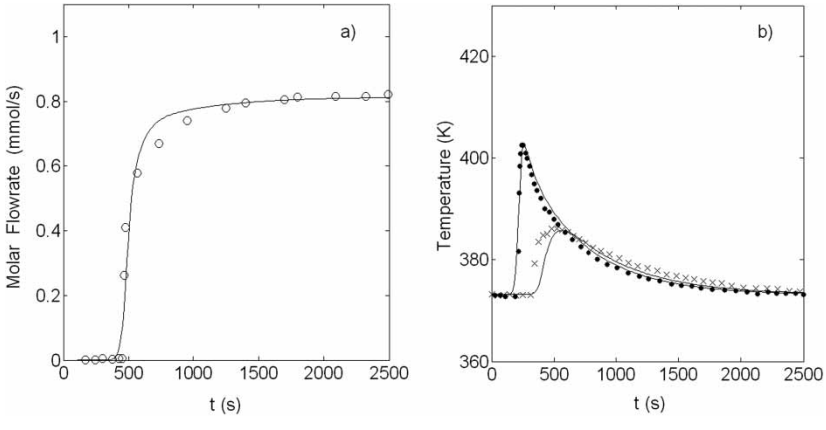

Figure 7. a) Experimental breakthrough curves of propane (○) on 13X zeolite initially activated with nitrogen; b) gas temperature histories at the middle bed (●) and wall column temperature histories at the top of the bed (×) during the adsorption of propane. Solid lines are simulations obtained with the non-isothermal bidisperse model. ($Q = 1.0$ SLPM; $P = 1.5$ bar; $T = 373$ K).

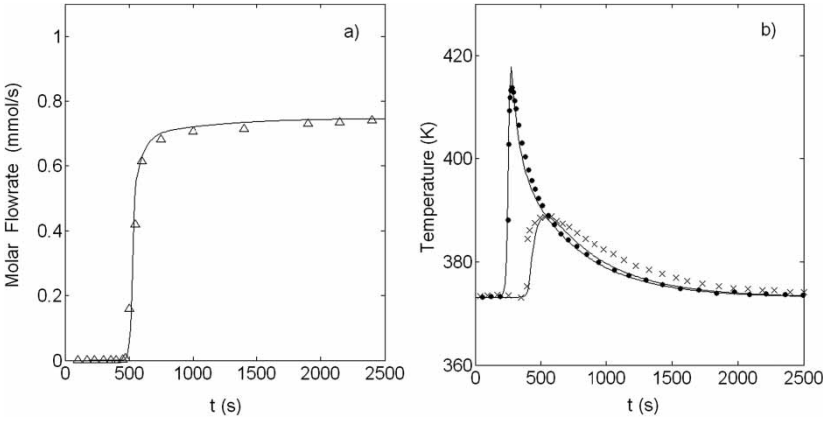

Figure 8. a) Experimental breakthrough curves of isobutane (△) on 13X zeolite initially activated with nitrogen; b) gas temperature histories at the middle bed (●) and wall column temperature histories at the top of the bed (×) during the adsorption of isobutane. Solid lines are simulations obtained with the non-isothermal bidisperse model. ($Q = 1.0$ SLPM; $P = 1.5$ bar; $T = 373$ K).

Adsorption and Desorption of Single Component over 13X Zeolite Saturated by Isobutane

Experimental adsorption and desorption runs were carried out in order to confirm that isobutane can displace and be displaced by both propane and propylene. At the same time, validation of the model is tested relative to the experiments made in a fixed bed, before to be included in the future simulated moving bed model.

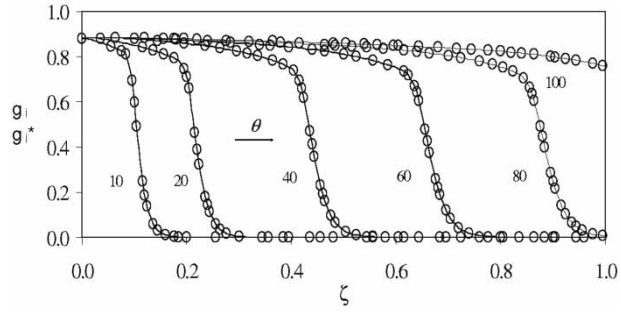

Figure 9. Simulated dimensionless concentration profile of isobutane in adsorbed phase (solid lines) and dimensionless equilibrium solid concentration (○) along the adsorption fixed bed at different dimensionless times θ.

Propylene-Isobutane System

Before performing some breakthrough experiments with a propane-propylene mixture, it is essential to study the dynamic behavior of pure component in presence of isobutane. Figures 10 and 11 show breakthrough curve of propylene during the adsorption and desorption steps respectively. On the same figures are also represented the gas and wall temperature histories predicted by the bidisperse control model with the respective experimental run. It is observed in Fig. 10 that isobutane is displaced very easily by propylene. The breakthrough curves are considerably abrupt seeing that the adsorption isotherm of propylene is highly favorable. Moreover, a small drop of isobutane molar flowrate can be seen at the beginning with a significant thermal peak due to the isobutane displacement by adsorption of a species like propylene with a higher adsorption enthalpy. Conversely, in Fig. 11 the propylene desorption presents a typical roll-up during the isobutane adsorption with very broad and tailing breakthrough curves. A consequence of these dispersive curves is the long time required to complete desorption. Considering the temperatures histories, a thermal well is noted because of the smaller heat of adsorption of isobutane. It is worthwhile to note that all these phenomena of roll over are linked up to the velocity variation along the bed. These results can be explained with the single gas adsorption isotherms measured and presented in the previous section. In fact, it appears by analyzing the adsorption isotherms that propylene is much more adsorbed than isobutane at 373 K and 150 kPa, with 2.2 and 1.55 mol/kg of

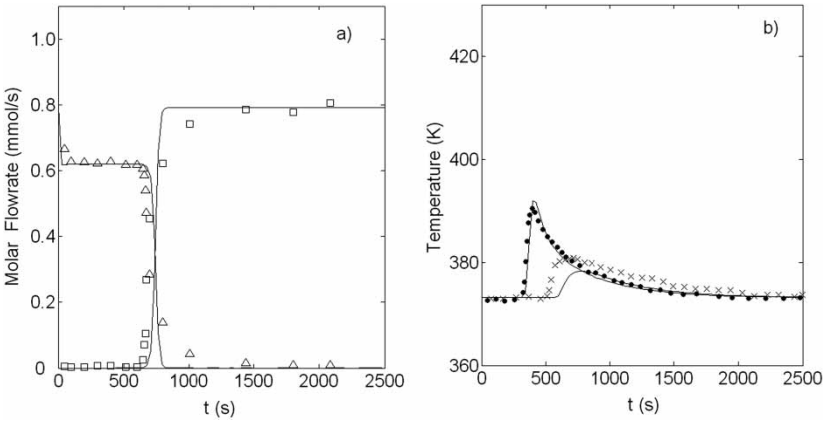

Figure 10. a) Experimental propylene (□) breakthrough curves on 13X zeolite initially saturated with isobutane (△); b) gas temperature histories at the middle bed (●) and wall column temperature histories at the top of the bed (×) during the adsorption of pure propylene. Solid lines are simulations obtained with the non-isothermal bidisperse model. ($Q = 1.0$ SLPM; $P = 1.5$ bar; $T = 373$ K).

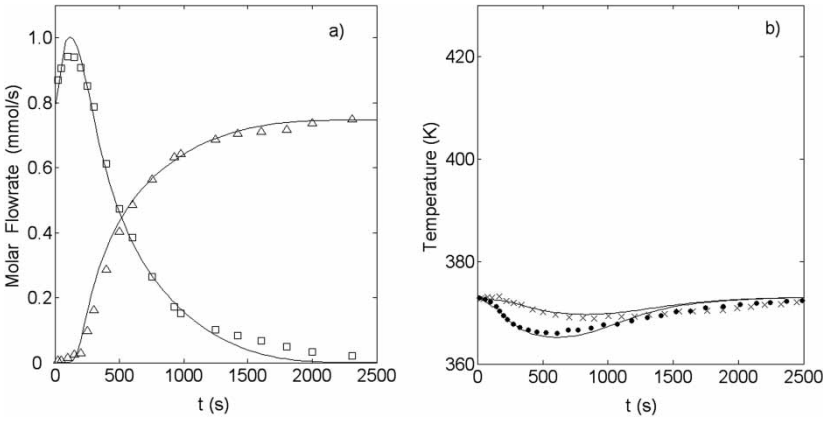

Figure 11. a) Experimental propylene (□) blowdown curves on 13X zeolite by adsorption of isobutane (△); b) gas temperature histories at the middle bed (●) and wall column temperature histories at the top of the bed (×) during the desorption of pure propylene. Solid lines are simulations obtained with the non-isothermal bidisperse model. ($Q = 1.0$ SLPM; $P = 1.5$ bar; $T = 373$ K).

adsorbed amount respectively. Thus, an empiric rule can be established according to these experiments and a positive roll-up of the more adsorbable species is expected when this one is displaced by a less adsorbable component. On the other hand, a significant drop of the less adsorbable gas can be assumed if it is displaced by a more adsorbable one. In terms of desorption time, it is clearly shown than isobutane desorbs faster than propylene in reciprocal bed saturation conditions.

Propane-Isobutane System

Figures 12 and 13 show the adsorption and desorption of propane through a fixed bed adsorbent saturated and regenerated with isobutane. One can observe that the exit molar flowrate breakthrough curves of propane adsorption is dispersive while its desorption breakthrough curve by flowing isobutane is sharper. This observation was also expected due to the isobutane equilibrium isotherm which is more favorable than propane in adsorption and becomes unfavorable during its desorption by propane. Therefore, the breakthrough time is faster in the case of isobutane adsorption ($t_s \sim 500$ sec). Regarding the temperature histories, a negligible gas and wall column temperature variation both for propane and isobutane adsorption is observed. The isothermicity can be explained by a compensation of the energy released during both adsorption and desorption of the two species. In fact the energy released per kilogram of adsorbent during the adsorption of propane is around $+64$ kJ/kg and is very closed to the energy discharged during the desorption of isobutane -65 kJ/kg. These values are the product

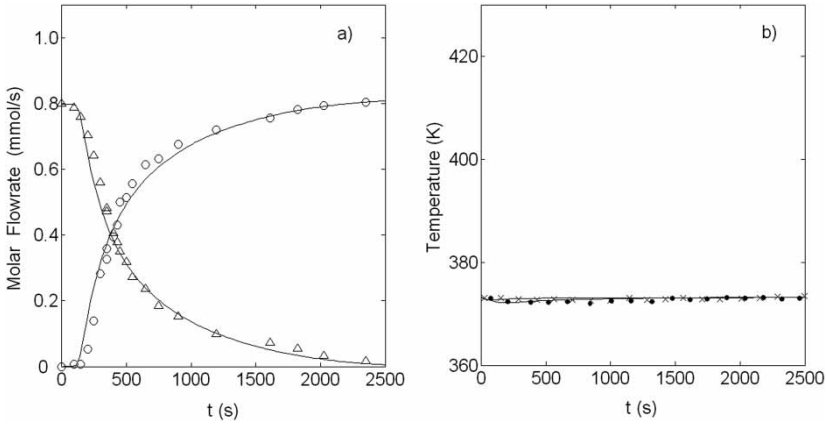

Figure 12. a) Experimental propane (○) breakthrough curves on 13X zeolite initially saturated with isobutane (△); b) gas temperature histories at the middle bed (●) and wall column temperature histories at the top of the bed (×) during the adsorption of pure propane. Solid lines are simulations obtained with the non-isothermal bidisperse model. ($Q = 1.0$ SLPM; $P = 1.5$ bar; $T = 373$ K).

of the heat of adsorption of propane and the loading of propane at the feed condition and the heat of desorption of isobutane multiplied by the initial loading of isobutane, respectively. It should also be noted that these results are in good agreement with the previous studies regarding the linear variation of heat of sorption with carbon number (30–32).

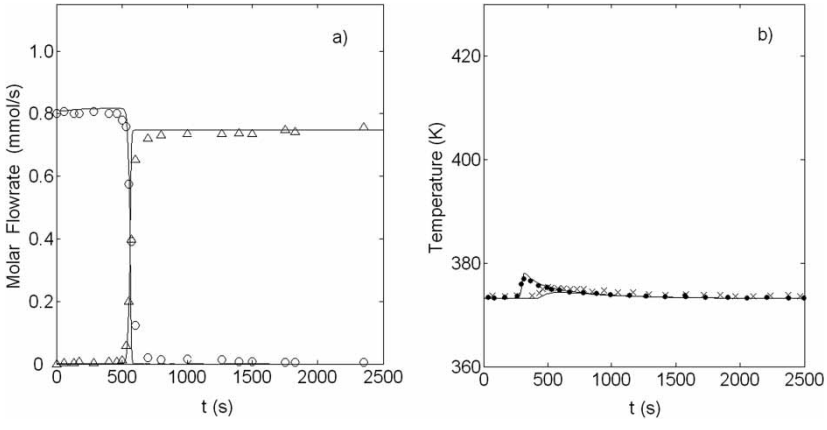

Figure 13. a) Experimental propane (○) blowdown curves on 13X zeolite by adsorption of isobutane (△); b) gas temperature histories at the middle bed (●) and wall column temperature histories at the top of the bed (×) during the desorption of pure propane. Solid lines are simulations obtained with the non-isothermal bidisperse model. ($Q = 1.0$ SLPM; $P = 1.5$ bar; $T = 373$ K).

Again, model predictions of the breakthrough curves are in close agreement with all experimental results shown in Figs. 10 to 13 corresponding to the different binary systems. The value of the parameter concerning heat transfer at the wall was determined in order to match the experimental curves, which ranges from 30 to 60 W/m^2K. It is noteworthy that the values of overall heat transfer coefficient and wall specific heat were fixed at 30 $W/m^2 \cdot K$ and 500 $J \cdot kg^{-1} \cdot K^{-1}$ for all the simulated breakthrough curves.

Adsorption and Desorption of Propane-Propylene Mixture over 13X Zeolite Saturated by Isobutane

Figures 14 and 15 show the breakthrough curves and temperature histories of a propane (25%)/propylene (75%) mixture adsorption and desorption over a fixed bed adsorbent saturated and regenerated with isobutane. It is distinctly shown in Fig. 14 that isobutane is easily displaced from the zeolite with three main plateaus and two transitions, corresponding to propane and propylene adsorption respectively. The molar flowrate breakthrough curves of all the components are sharp and the temperature histories present a thermal peak due to the adsorption heat of propylene and its favorable equilibrium isotherm. The reverse experiment presented in Fig. 15, shows dispersive breakthrough curves and a thermal well as a consequence of the unfavorable propylene equilibrium isotherm for desorption. Moreover, two

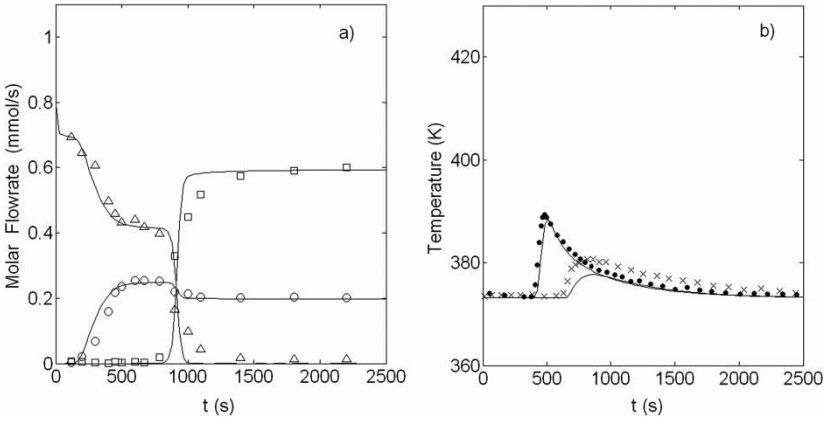

Figure 14. a) Breakthrough curves of propylene/propane mixture on 13X zeolite initially saturated with isobutane; b) gas temperature histories at the middle bed (●) and wall column temperature histories at the top of the bed (×) during the adsorption of the mixture. (□) Propylene, (○) Propane and (△) Isobutane. Solid lines are simulations obtained with the non-isothermal bidisperse model. (feed composition: 75% propylene − 25% propane $Q = 1.0$ SLPM; $P = 1.5$ bar; $T = 373$ K).

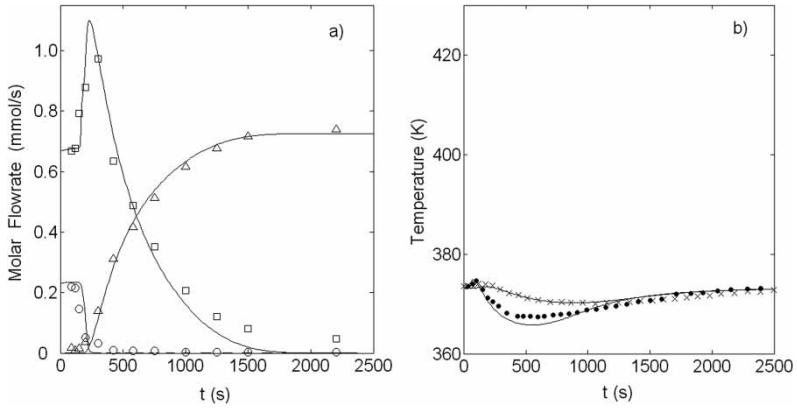

Figure 15. a) Blowdown curves of propylene/propane mixture on 13X zeolite by adsorption of with isobutane; b) gas temperature histories at the middle bed (●) and wall column temperature histories at the top of the bed (×) during the desorption of the mixture. (□) Propylene, (○) Propane and (△) Isobutane. Solid lines are simulations obtained with the non-isothermal bidisperse model. (feed composition: 75% propylene −25% propane $Q = 1.0$ SLPM; $P = 1.5$ bar; $T = 373$ K).

distinct plateaus can be seen for propylene desorption corresponding to the bed initial state and the feed state, respectively. It can be also observed that the breakthrough time is more important. Nevertheless, it appears markedly that isobutane succeeds in removing the mixture and principally propylene from the 13X zeolite.

From these last results, it can be concluded that the mathematical model proposed in this study provides a good representation of the experimentally observed behavior of exit molar flowrate breakthrough curves and temperatures histories.

CONCLUSION

New adsorption isotherms of propane, propylene, and isobutane over 13X zeolite have been measured by a gravimetric method and compared to the results reported previously in the literature. The adsorption of each pure gas on 13X zeolite extrudates packed in a fixed bed has been studied with different initial states regarding the activation or saturation of the adsorbent bed. Through multicomponent breakthrough experiments we observed that isobutane is able to displace propane, propylene, and their mixture from the 13X zeolite. Isobutane was itself fairly easily displaced from the adsorbent, so that the zeolite could be reused in a cyclic gas separation processes as a simulated moving bed for the separation of propane-propylene mixture. The mathematical model based on a double LDF approximation for the mass transfer, taking into

account a variable velocity along the fixed bed and including a heterogeneous energy balance was able to describe quite well the breakthrough curves and the temperature profiles obtained experimentally. This fixed bed adsorption model represents the heart of all cyclic processes modeling and, in the framework of this study, of the simulated moving bed model.

In the near future this detailed model, combined with the choice of isobutane as a desorbent, will be used to study the separation region of the propane-propylene mixture, and then to establish the optimal operating conditions for a SMB unit.

NOTATION

b	adsorption equilibrium constant $(-)$
Bi	Biot number (-)
C_0	total fluid phase concentration$(\mathrm{mol/m^3})$
$\tilde{C}_p$	molar specific heat at pressure constant of the gas mixture $(\mathrm{J/mol \cdot K})$
$\hat{C}_{pg}$	specific heat per kilogram of the gas mixture $(\mathrm{J/kg \cdot K})$
$\hat{C}_{pw}$	wall specific heat $(\mathrm{J/kg \cdot K})$
$\tilde{C}_v$	molar specific heat at volume constant of the gas mixture $(\mathrm{J/mol \cdot K})$
D_c	crystal diffusion coefficient $(\mathrm{m^2/s})$
D_{zm}	mass axial dispersion coefficient $(\mathrm{m^2/s})$
D_m	molecular diffusivity $(\mathrm{m^2/s})$
D_p	pore diffusivity $(\mathrm{m^2/s})$
F	dimensionless total fluid phase concentration $(-)$
F_i	dimensionless concentration of i component is the bulk phase $(-)$
$\bar{f}_i$	dimensionless average concentration of i component inside the pellet pores $(-)$
$\bar{\bar{g}}_i$	dimensionless average adsorbed concentration for i component in the pellet $(-)$
$\bar{g}_i^*$	dimensionless adsorbed phase concentration in the crystal in equilibrium with the gas inside the particule $(-)$
ΔH_i	isosteric heat of adsorption of i component $(\mathrm{J/mol})$
h_f	film heat transfer coefficient between gas and solid $(\mathrm{W/m^2 \cdot K})$
h_w	film heat transfer coefficient between gas and the wall $(\mathrm{W/m^2 \cdot K})$
k_g	gas thermal conductivity $(\mathrm{W/m \cdot K})$
K_m	mass transfer coefficient $(\mathrm{m/s})$
L	length of the column (m)
M	molecular weight $(\mathrm{g/mol})$
Nu	Nusselt number $(-)$

P	gas pressure (Pa)
Pe_h	mass Peclet number (−)
Pe_m	thermal Peclet number (−)
Pr	Prandtl number (−)
Q	volumetric flow rate (SLPM)
q_m	maximum loading capacity of the sorbent (mol/kg)
$\Re$	ideal gas constant (=8.3143 J/mol · K)
r_c	crystal radius (m)
Re	Reynolds number (−)
r_p	pore radius (m)
R_p	pellet radius (m)
Sc	Schmidt number (−)
Sh	Sherwood number (−)
T_g	gas temperature (K)
T_s	solid temperature (K)
T_w	wall temperature (K)
t	time variable (s)
U	overall heat transfer coefficient (W/m^2K)
v_0	superficial velocity (m/s)

Greek Letters

ε_b	bulk porosity (−)
ε_p	pellet porosity (−)
λ	heat axial dispersion coefficient (W/m · K)
η	viscosity (Pa · s)
ρ	fluid density (kg/m^3)
ρ_b	bulk density (kg/m^3)
ρ_p	pellet density (kg/m^3)
τ	tortuosity (−)
θ	dimensionless time

Superscripts

*	equilibrium; dimensionless parameter
-	volumetric average
$=$	double volumetric average
$\sim$	per mole
$\wedge$	per kilogram

Subscripts

c	crystal
g	gas

i,j	species in binary system
o	reference feed condition
p	pellet; constant pressure
s	solid
v	constant volume
w	wall

Abbreviations

LDF	Linear driving force
ODE	Ordinary differential equations
OCFEM	Orthogonal collocation in finite elements method
ODAE	Ordinary differential and algebraic equations
PDAE	Partial differential and algebraic equations
PDE	Partial differential equation
PSA	Pressure swing adsorption
SMB	Simulated moving bed
VSA	Vacuum swing adsorption

ACKNOWLEDGMENTS

This work was carried out at LSRE with a financial support from IFP (Institut Français du Pétrole). N.L. gratefully acknowledges the grant from Association Nationale de la Recherche Technique (Research fellowship: CIFRE 518/2004).

REFERENCES

1. Eldridge, R.B. (1993) Olefin/paraffin separation technology: a review. *Ind. Eng. Chem. Res.*, 32 (10): 2208.
2. Bryan, P.F. (2004) Removal of propylene from fuel-grade propane separation and purification review 33 (2): 157–182.
3. Ghosh, T.K., Lin, H.-D., and Hines, A.L. (1993) Hybrid adsorption-distillation process for separating propane and propylene. *Ind. Eng. Chem. Res.*, 32 (10): 2390.
4. Manley, D.B. and Swift, G.W. (1971) Relative volatility of propane-propene system by integration of general coexistence equation. *J. Chem. Eng. Data*, 16 (3): 301.
5. Kumar, R., Golden, T.C., White, T.R., and Rokicki, A. (1992) Novel adsorption distillation hybrid scheme for propane/propylene separation. *Sep. Technol.*, 15: 2157.
6. Safarik, D.J. and Eldridge, R.B. (1998) Olefin/paraffin separations by reactive absorption: A Review. *Ind. Eng. Chem. Res.*, 37: 2571.
7. Da Silva, F.A. and Rodrigues, A.E. (2001) Propylene/propane separation by VSA using 13X zeolite. *AIChE J.*, 47 (2): 341–357.

8. Da Silva, F.A. and Rodrigues, A.E. (2001) Vacuum swing adsorption for propylene/propane separation with 4A zeolite pellets. *Ind. Eng. Chem. Res.*, 40 (24): 5758–5774.
9. Grande, C.A. and Rodrigues, A.E. (2005) Propane/propylene separation by pressure swing adsorption using zeolite 4A. *Industrial & Engineering Chemistry Research*, 44: 8815–8829.
10. Rege, S.U. and Yang, R.T. (2002) Propylene/propane separation by PSA: sorbent comparison and multiplicity of cyclic steady states. *Chem. Eng. Sci.*, 57: 1139–1149.
11. Broughton, D.B. and Gerhold, C.G (1961) Continuous Sorption Process Employing Fixed bed of Sorbent and Moving Inlets and Outlets. U.S. patent 2,985,589.
12. Rao, D.P., Sivakumar, S.V., and Ramaprasad, B.S.G. (2005) Novel simulated moving-bed adsorber for the fractionation of gas mixtures. *Journal of Chromatography A*, 1069 (1): 141–51.
13. Grande, C.A., Gigola, C., and Rodrigues, A.E. (2002) Adsorption of propane and propylene in pellets and crystals of 5A zeolite. *Industrial & Engineering Chemistry Research*, 41: 85–92.
14. Grande, C.A. and Rodrigues, A.E. (2004) Adsorption kinetics of propane and propylene in zeolite 4A. *Chemical Engineering Research and Design*, 82: 1604–1612.
15. Grande, C.A., Araújo, J.D.P., Cavenati, S., Firpo, N., Basaldella, E., and Rodrigues, A.E. (2004) New π-complexation adsorbents for propane-propylene separation. *Langmuir*, 20: 5291–5297.
16. Järvelin, H. (1990) *Adsorption of Propane and Propylene*; Tech. Rep. SRP Doc., No. F-90-4, Separation Reasearch Program: the University of Texas, USA.
17. Hyun, S.H. and Danner, R.P. (1982) Equilibrium adsorption of ethane, ethylene, isobutane, carbon dioxide, and their binary mixtures on 13X molecular sieves. *J. Chem. Eng. Data*, 27: 196–200.
18. Valenzuela, D.P. and Myers, A.L. (1989) *Adsorption Equilibrium Data Handbook*; Prentice-Hall: New York, USA.
19. Rodrigues, A.E., Lamia, N., Grande, C.A., Wolff, L., Leflaive, P., and Leinekugel-le-Coq, D. Procédé de Séparation du Propylène en Mélange avec du Propane par Adsorption en Lit Mobile Simulé en Phase Gaz ou Liquide utilisant une Zéolithe de type Faujasite 13X comme Solide Adsorbant. FR. Patent pending 06-06827, July, 2006.
20. Toth, J. (1971) State equations of the solid-gas interface layers. *Acad. Sci. Hung.*, 69 (3): 311.
21. Sircar, S. (1991) Role of adsorbent heterogeneity on mixed gas adsorption. *Ind. Eng. Chem. Res.*, 30: 1032.
22. Reid, R.C., Prausnitz, J.M., and Poling, B.E. (1987) *The Properties of Gases and Liquids*, 4th edn.; McGraw-Hill: NY., USA.
23. Wakao, N. and Funazkri, T. (1978) Effect of fluid dispersion coefficients on particle-to-Fluid mass transfer coefficients in packed beds. *Chem. Eng. Sci.*, 33: 1375–1384.
24. Da Silva, F.A., Silva, J.A.C., and Rodrigues, A.E. (1999) A general package for the simulation of cyclic adsorption processes. *Adsorption*, 5: 229–244.
25. Brandani, S., Hufton, J., and Ruthven, D.M. (1995) Self-diffusion of propane and propylene in 5A and 13X zeolite crystals studied by the tracer ZLC method. *Zeolites*, 15: 624–631.

26. Da Silva, F.A. and Rodrigues, A.E. (1999) Adsorption equilibria and kinetics for propylene and propane over 13X and 4A zeolite pellets. *Ind. Eng. Chem. Res.*, 38: 2051–2057.
27. Ruthven, D.M. and Loughlin, K.F. (1972) The diffusional resistance of molecular sieve pellets. *Can. J. Chem. Eng.*, 28: 550–552.
28. Silva, J.A.C. and Rodrigues, A.E. (1996) Analysis of ZLC technique for diffusivity measurements in bidisperse porous adsorbent pellets. *Gas. Sep. Purif.*, 10 (4): 207–224.
29. Silva, J.A.C. and Rodrigues, A.E. (1997) Sorption and diffusion of n-pentane in pellets of 5A zeolite. *Ind. Eng. Chem. Res.*, 36: 493–500.
30. Barrer, R.M. and Sutherland, J.W. (1956) Inclusion complexes of faujasite with paraffins and permanent gases. *Proc. R. Soc.*, 237: 439–463.
31. Stach, H. (1979) *Thermodynamics of Adsorption of n-Paraffins on NaX Zeolites*; Paper No 7; Preprint of Workshop Adsorption of Hydrocarbons in Zeolites: Berlin: Germany.
32. Calero, S., Dubbeldam, D., Krishna, R., Smit, B., Vlugt, T.J.H., Denayer, J.F.M., Martens, J.A., and Maessen, T.L.M. (2004) Understanding the role of sodium during adsorption: a force field for alkanes in sodium exchanged faujasites. *J. Am. Chem. Soc.*, 126: 11377–11386.